KKU Res. J. 2012; 17(3):348-357
http : //resjournal.kku.ac.th

Shrinking Size Effects of CPP–TMR and CPP–GMR Heads: Failure Phenomena Caused by Electrostatic Discharge

*Kanuengnit Marongmued and Chiranut Sa-ngiamsak**

Department of Electrical Engineering, Faculty of Engineering, Khon Kaen University, Thailand
**Correspondent author: chiranut@kku.ac.th*

Received February 20, 2012
Accepted June 1, 2012

Abstract

This work presents the tolerance of CPP-TMR and CPP-GMR heads to ESD events when the sizes of both reader technologies are shrinking. The shrinking size effect actually indicates the growth of AD targeting to Tb/in^2. Blocking temperature, melting temperature, and electric field breakdown of the oxide layer are the key parameters for investigation upon the temperature increment of CPP-TMR and CPP-GMR heads caused by an ESD current. The investigation was carried out by using a finite element analysis, solver and simulation software. The results reveal that at 30% shrinking size, CPP-TMR is 15% less tolerance to ESD phenomena than that of CPP-GMR technology for the case of hard failure aspect. On the other hand, CPP-GMR is approximately 10% more sensitive to ESD events than CPP-TMR technology for the case of soft failure aspect.

Keywords: magnetoresistance, current perpendicular, electrostatic discharge, shrinking, failure

1. Introduction

The hard disk drive (HDD) industry has been facing strong competition from other data storage devices such as solid state drive. In order to keep HDD's advantages in cost and capacity, the areal density (AD) should maintain an annual growth rate of 30% to 40%. Nowadays research and development capability (R&D) has been working on 1 Tb/in^2. 10 Tb/in^2 is the target in year 2015. The increase of AD results in smaller bit size of a head reader. These days HDD industry has been employing tunnel magnetoresistance (TMR) as a sensor to read back data recorded in magnetic media due to its high TMR ratio is over 100%; however,TMR head has been predicted to reach the limitation of 2 Tb/in^2 recording density, because of its high impedance. Predictably, giant magnetoresistance (GMR) reader using all metallic materials and in current perpendicular to the plane (CPP) geometry has to be employed for Tb/in^2(1).

GMR sensors are highly susceptible to be damaged byelectrostatic discharge (ESD) event; therefore it is necessary to characterize the ESD damage thresholds and mechanism failure of these devices using three standard models: Human Body Model (HBM), Machine Model (MM), and Charged Device Model (CDM) (2). ESD damage modes upon GMR can be classified into three types, namely hard ESD damage, soft ESD damage, and quasi-ESD damage as summarized in Table 1.

Table 1. Classification of ESD effects on GMR heads(3).

	Mode	Phenomena
Hard ESD	Mechanical breakdown or melting and diffusion in strip of GMR head	Melting
		Diffusion
Soft ESD	Magnetic destruction	Defect in Permanent Magnet
		Defect in Free layer
		Defect in Pin layer
		Defect in AFM
		Otherwise
Quasi ESD	GMR is normal	Capacitance coupling ESD
		EMI

1.1 Hard ESD damage

Hard ESD damage is defined as a mode where GMR elements are mechanically damaged by melting or insulating damage. Moreover, inter-diffusion is also defined as hard ESD which caused by a metal-contact during an HGA process. Melting of spacer layer (copper) has been most commonly found for this type of failure. The prime parameter to monitor this case is the melting temperature of space material (T_M).

1.2 Soft ESD damage

GMR heads still operate as normal; however, occasionally, its performance is degraded under the relatively high stress of write current or long term usage. ESD soft damage can be defined as a mode where a GMR is suffered from magnetic damage with no change or very small change in resistance (3). That is commonly found degradation of magnetic properties in anti-ferromagnetic (AFM) layers. The prime parameter is the blocking temperature (T_B). T_B is the threshold temperature where the moment or magnetization of material is blocked; and T_B depends on particle size and timescale of observation. Larger particles have higher blocking temperatures. The longer the observation time last it is more likely that the magnetic moment can be reversed. Mostly, the blocking temperature is lower than the melting temperature.

The failure of GMR heads caused by ESD events has been well studied and understood; however, it is otherwise with CPP-TMR heads. Basically, there are two failure modes for an insulator barrier of CPP-TMR heads under bias voltage or current. The failure caused by the pinhole growth is known as extrinsic breakdown while the intrinsic breakdown is the failure of the pinhole-free barrier. The extrinsic breakdown process may be easily imaged, but the intrinsic breakdown has not yet been adequately understood. Two theories have been proposed to illustrate the intrinsic breakdown. One is the E-model theory, relating the breakdown to the defect generation caused by distortion and breaking of the ionic bonds under the electric field. The other one believes that the tunneling current creates defects, which in return enhances the tunneling current (4).

This work presents the tolerance of CPP-TMR and CPP-GMR heads to ESD events when the sizes of both reader technologies are shrinking. The shrinking size effect actually indicates the growth of AD targeting to Tb/in^2. Three prime parameters: Blocking temperature (T_B), Melting temperature (T_M), and Electric field breakdown (E_B) of the oxide layer are the key parameters for our investigation upon the temperature increment of CPP-TMR and CPP-GMR heads caused by ESD current.

2. Research Methodology

The investigation upon the effects of ESD peak current in soft and hard damage was carried out by applying DC current from top to bottom of read head structures by using finite element simulation (FEM) program. The temperature of important layers, interfaces between pinned and pinning,and electric field across oxide barrier were carefully captured in order to investigate the physical failure of the reader through the critical parameters of those three important at the same time. Critical temperatures and electric field breakdown indicating the threshold current level of both soft and hard failures at significant layers is shown in Table 2. The simulation was conducted with CPP-TMR and CPP-GMR head technologies by shrinking reader size from 5% to 30% in 3-D. Both read head technologies havean identical active area of rectangular shape and lateral size with 80 nm (W) x 120 nm (L), created with triangular mesh and ambient temperature was set at 300K (26.85 ºC).

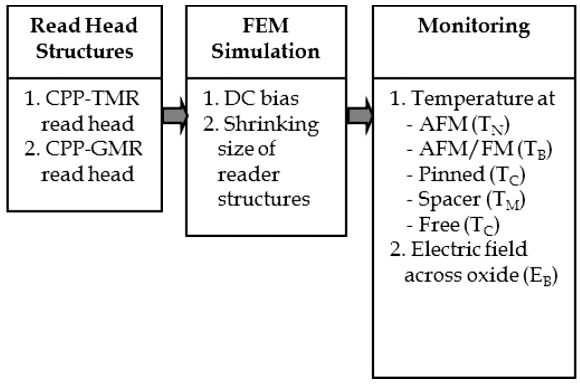

Figure 1. Flow chart of research methodology.

Table 2. Important parameters and its critical value (5-7).

Layer	Critical Value	Detail
FM/AFM	170 ºC	Blocking Temperature (T_B)
AFM	420 ºC	Neel Temperature (T_N)
FM	520 ºC	Curie Temperature (T_C)
Copper	1043 ºC	Melting Temperature (T_M)
Oxide	12 MV/cm	Electric Field Breakdown (E_B)

3. Structures and Modeling

3.1 CPP-TMR and CPP-GMR structure

The profile of CPP-TMR and CPP-GMR head used for the simulation was taken from several publications being used as an example to identify the shrinking effect upon both technologies. The layer structures are depicted in Table 3.

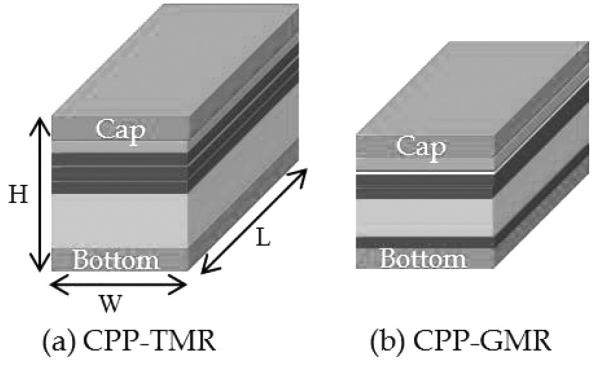

Figure 2. Structures of (a) CPP-TMR and (b) CPP-GMR read heads.

Table 3. Device dimension and material used for simulator (8-9).

Technology	CPP-TMR		CPP-GMR	
Layer	**Material**	**Thickness (nm)**	**Material**	**Thickness (nm)**
Cap	Ta	9	Ta	5
Free	NiFe	7	NiFe	3.5
	CoFe	5	CoFe	1
Spacer	Mgo	0.9	Cu	2.8
Pinned	CoFe	4	CoFe	3
	Ru	0.6	Ru	0.9
	CoFe	4	CoFe	3.4
Pinning	IrMn	25	IrMn	7
Bottom	Ta	9	Ru	2
			Ta	5
Total Height	64.5		33.6	

3.2 Electro-Thermal Model

The heat resulted of the current passing through the material is caused by Joule Heating that given by:

$$Q = \frac{1}{\sigma} |J|^2 = \sigma |\nabla V|^2 \quad 1)$$

where

Q is the Joule heat induced by current pulse

σ is the electric conductivity

J is the electric current density

V is the electric potential

The thermal conduction and the temperature of reader layers triggered by Joule heat are determined by

$$Q = \rho c \frac{\partial T}{\partial t} - \nabla \cdot (k \nabla T) \quad 2)$$

where

ρ is the densityof material

T is the temperature

c is the heat capacity

k is the thermal conductivity

t is the time

Q is the heat flux

The electric field (E) across the layer was caused by the current density *J* given by:

$$J = \sigma E = -\sigma \nabla V \quad 3)$$

4. Simulations and Discussions

The investigation was carried out by using finite element analysis, solver and simulation software COMSOL Multiphysics®. The emulated ESD current was injected into CPP-TMR and CPP-GMR structures and the temperature profile and heat distribution along the reader heads were investigated and captured as shown in Figure 3.

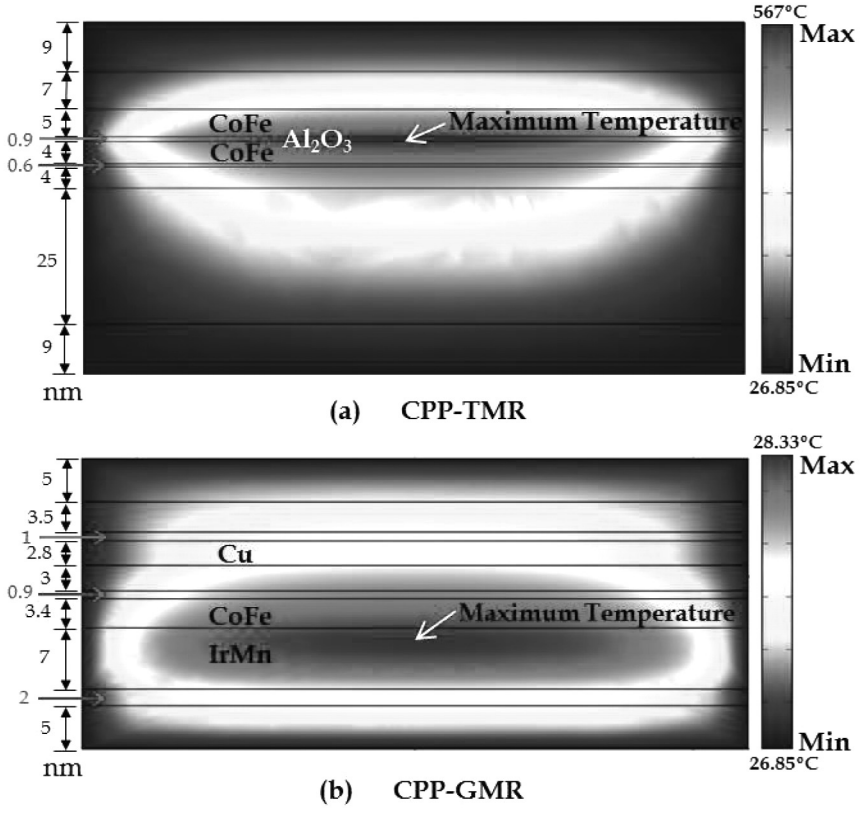

Figure 3. (Color line) (a) Temperature profile of CPP-TMR sensor induced by current. (b) Temperature profile of CPP-GMR sensor induced by current.

Figure 3 shows temperature profile at each layers of both CPP-TMR and CPP-GMR read head. The simulation results clearly identify the location of the highest temperature which occurs at the spacer layer for CPP-TMR head and pinning layer for CPP-GMR head. The highest temperature of CPP-TMR head induced by current occurs at the oxide barrier due to the highest heat capacity and the lowest electrical conductivity compare with other layers. On the other hand, the CPP-GMR sensor induces the highest Joule Heating at the IrMn layer due its high electrical resistivity and highest thickness compare to other thin film. Figure 4 shows more clearly temperature increment in CPP-TMR and CPP-GMR read heads attacked by ESD peak current. The simulation of heat distribution of both technologies suggest that the thickness of the pinned layers (multiple layers) of CPP-GMR heads can delay or absorb Joule heating mainly occurred at the antiferromagnetic (AFM) layer, apart from behaving as a magnetic pin on the reference layer. The temperature profile of both structures provides an insight to an initial location of physical damage of the reader technology.

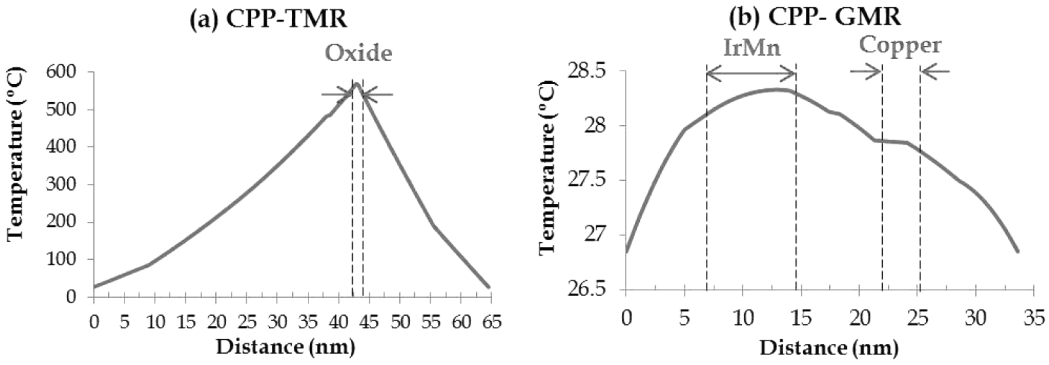

Figure 4. Temperature distribution of cross-section (a) CPP-TMR and (b) CPP-GMR zapped with ESD current of 10 mA.

The temperature of the listed layer as shown in Table 3 were monitored and captured. The effect of size shrinking of the head technology was simulated by reducing the dimension of the head structures in all three dimensions while the critical temperature at important layers, at the interfaces, and electric filed across oxide barrier were carefully observed. The normalized threshold current of CPP-TMR and CPP-GMR were plotted in Figure 5 and Figure 6, respectively.

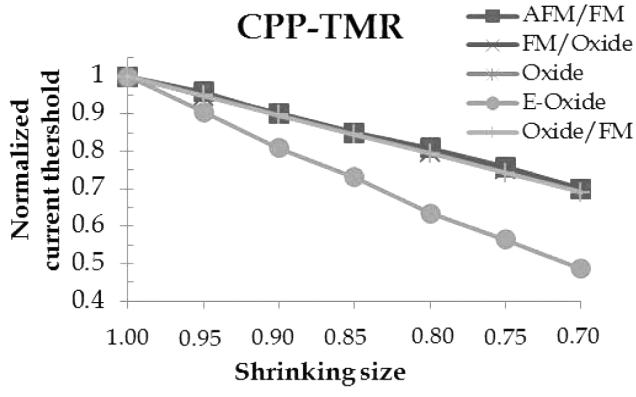

Figure 5. Normalization of critical current in CPP-TMR read heads.

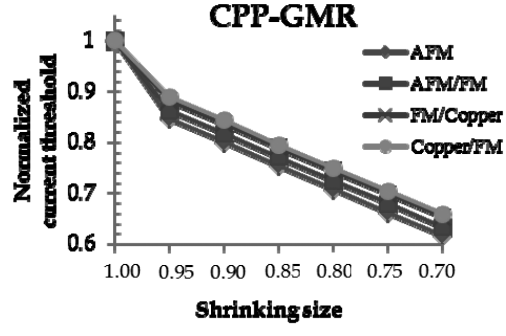

Figure 6. Normalization of critical current in CPP-GMR read heads.

Figure 5 and Figure 6 show a normalized critical current resulting in a malfunctioned read head while shrinking size of read head in 3-Dwith the reduction step of 5%. In case of CPP-TMR technology, the critical current induced temperature of interested layers to critical level that reflecting softfailure such as T_N, T_B, T_C are linearly reduced. The temperature at ferromagnetic layer such as free layer and pinned layer reach T_C causing the magnetic property of ferromagnetic becoming paramagnetic while the antiferromagnetic deteriorate to paramagnetic material when the temperature reach T_N. Both cases are an example of changing of magnetic property. The important parameter located at the interface between the pinned and the pinning layers are blocking temperature T_B. Once the temperature at the interface reaches T_B then the magnetization of pinned layer is free to switchor in the other worda loose of exchange bias. Interestingly, when the size of TMR heads being shrunk the falling of threshold current causing the hard failure of CPP-TMR heads due to an oxide barrier breakdown is 1.7 time faster than the case of soft failure aspectwhile the critical current of key layers to reach T_N, T_B, T_C, and T_M of CPP-GMR headsare linearly reduced in a similar rate. The resilience to hard failure and soft failure caused by an induced current of CPP-TMR vs CPP-GMR is shown in Figure 7 and Figure 8, respectively.

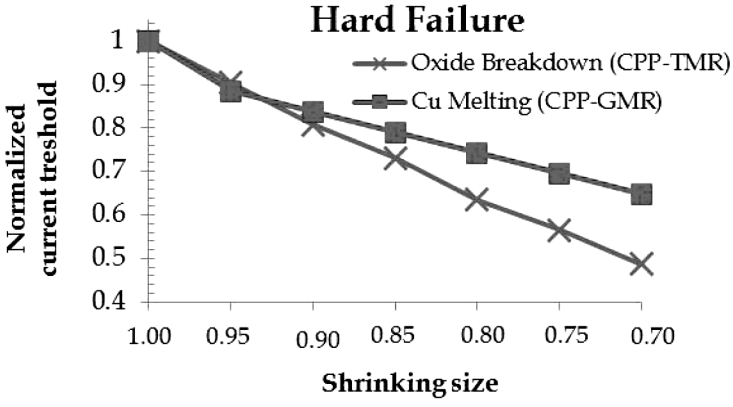

Figure 7. Normalization of critical current for hard failure in both CPP-TMR and CPP-GMR read heads.

Comparison of the critical current level causing hard failure phenomena of CPP-TMR vs CPP-GMR head technologies is depicted in Figure7. The results clearly reveal the weakness of CPP-TMR heads comparing with CPP-GMR headsagainstan ESD event considering a shrinking effect. The threshold current of CPP-TMR is falling sharper than that of CPP-GMR; thus CPP-TMR heads are likely to fall into category of hard failure to ESD event rather than CPP-GMR when the size of the reader area is being shrunk.The physical damage or hard failure of CPP-TMR is caused by electric field exceeding the oxide (MgO) break down level while that of CPP-GMR is caused by Joule heating exceeding the melting temperature of the conductive spacer. Shrinking size of the reader increases the current density (J) at the same current level. Considering Ohm's law in equation 3), current density (J) and electric field (E) both are sensitive to dimension of the reader while the Joule heating equations 1) – 2) only J is a function of cross section area of an active area. Moreover, the location of maximum temperature of CPP-GMR is at the AFM layer hence Joule heating at the AFM layer is dissipated and drops in temperature at the spacer layer (conductor). In conclusion, the CPP-TMR is more sensitive to the shrinking size effect than the case of CPP-GMR.

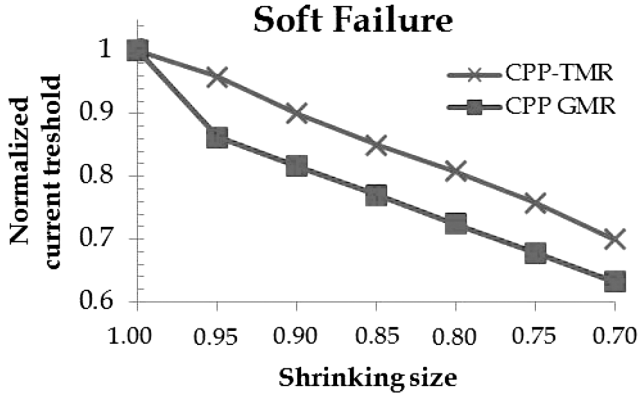

Figure 8. Normalization of critical current for soft failure in both CPP-TMR and CPP-GMR read heads.

Comparison of the critical current level causing soft failure phenomena of CPP-TMR vs CPP-GMR head technologies is depicted in Figure 8. The blocking temperature T_B is a critical parameter to consider the soft-failure threshold current level. The comparison was conducted with the same size and dimension of both technologies with identical shrinking scale. The results reveal that the critical current level of CPP-GMR is lower than that of CPP-TMR.The temperature increment at the pinned/pinning interface of both technologies depends on Joule heating; however the threshold current causing a soft damage of CPP-GMR is less than that of CPP-TMR, because the maximum temperature of CPP-GMR takes place at the pinning layer made of AFM material, particularly near the interface between the pinning and the pinned layers made of ferromagnetic (FM) material while CPP-TMR takes place at the oxide layer. Considering the Joule heating at the oxide layer of TMR being dissipated to AFM/FM interface is less than the case of CPP-GMR where the maximum temperature is located at the near AFM/FM interface. This indicates CPP-GMR heads will experience a soft failure phenomenon due to the temperature reaching T_B more than CPP-TMR heads.

5. Conclusions

The results conclude that at 30% shrinking size, CPP-TMR is 15% less tolerance to ESD phenomena than CPP-GMR technology for the case of hard failure. On the other hand, CPP-GMR is approximately 10% more sensitive to ESD event than CPP-TMR technology for the case of soft failure case.

6. Acknowledgement

Authors thank National Electronics and Computer Technology Center (NECTEC), National Science and Technology Development Agency (NSTDA), Seagate Technology (Thailand) Ltd., Industry/University Cooperative Research Center (I/UCRC) in Advanced Manufacturing, Institute of FIeld roBotics (FIBO), King Mongkut's University of Technology Thonburi University and Faculty of Engineering, Khon Kaen University.

7. References

(1) Han GC, Qiu J J, Wang L, Yeo WK, Wang CC. Perspectives of Read Head Technology for 10 Tb/in^2 Recording. Magnetics, IEEE Transactions on. 2010;46(3): 709-14.

(2) Lai TWY,Wallash A.Effect of GMR Recording Head Resistance on Human Body and Machine Model ESD Waveforms.Proceeding of the 24thE-OS/ESD symposium;2002 Oct 6-10; Charlotte, North Carolina, USA. ESD Association;2002. P. 340-4.

(3) Matsugi J, Nakano T, Mizoh Y, Nakamura K, Sakakima H.ESD Phenomena in GMR Heads in the Manufacturing Process of HDD and GMR Heads. Proceeding of the 25thEOS/ESD symposium;2003 Sept 21-25; Las Vegas, Nevada, USA. ESD Association;2003. P. 1-7.

(4) Yang T, Otagiri M, Kanai H, Uehara Y.Barrier degradation of tunneling magnetoresistance device with MgO barrier and low resistance-area product. JMagn and Magn Mat. 2010; 322(19): L53-56.

(5) Lombard L, Gapihan E, Sousa RC, Dahmane Y, Conraux Y, Portemont C, et al. IrMn and FeMn blocking temperature dependence on heating pulse width. JAppl Phys. 2010;107(9): 09D728.

(6) Fernandez-Outon LE, O'Grady K, Oh S, Zhou M, Pakala M.Large Exchange Bias IrMn/CoFe for Magnetic Tunnel Junctions.IEEE Trans Magn.2008;44(11): 2824-27.

(7) Paulsen JA, Lo CCH, Snyder JE, Ring AP, Jones LL, Jiles DC. Study of the Curie Temperature of Cobalt Ferrite Based Composites for Stress Sensor Applications.IEEE Trans Magn39(5): 3316–18.

(8) Ventura J, Ferreira R, Sousa JB, Freitas PP.Dielectric Breakdown in Underoxidized Magnetic Tunnel Junctions: Dependence on Oxidation Time and Area.IEEE Trans Magn.2006;42(10): 2658–60.

(9) Fuji Y, Yuasa H, Fukuzawa H.Formation of a nanobarrel structure in CPP-GMR spin-valve films. J Magn and Mag Mat. 2010;322(9-12): 1449–51.